

Mixing in a coastal environment:

2. A view from microstructure measurements

Neil S. Oakey and Blair J. W. Greenan

Department of Fisheries and Oceans (Canada), Bedford Institute of Oceanography, Dartmouth, Nova Scotia, Canada

Received 5 November 2003; revised 14 June 2004; accepted 10 August 2004; published 26 October 2004.

[1] During the Coastal Mixing and Optics Experiment in 1996 and 1997, an integrated dye and microstructure experiment was done to measure and compare mixing rates on the continental shelf. The results of the dye experiment are presented in the companion paper by *Ledwell et al.* [2004]. In this paper, we explore the results from microstructure measurements using a vertical profiling instrument. We measure temperature and velocity microstructure and, along with simultaneous measurements of salinity and temperature as well as a shipboard acoustic Doppler current profiler (ADCP), are able to estimate the vertical diffusivities of heat, mass, and momentum. In three of four dye injections performed, we were able to make a comparison of the diffusivity from both dye and microstructure measurements. Although the mixing rates were quite small (vertical diffusivity of heat, $K_T < 10^{-5} \text{ m}^2 \text{ s}^{-1}$), the two techniques yielded consistent results. A comparison of the vertical diffusivities K_T and K_ρ (the vertical diffusivity for density) allowed us to determine a flux Richardson number of $R_f = 0.16 \pm 0.03$. R_f showed little dependence on either the buoyancy frequency, N , or gradient Richardson number, R_i . A clear relationship was found between the ratio of diffusivities, K_m/K_T and R_i consistent with $K_m/K_T = 5 R_i$. Turbulence levels were extremely low, with Cox numbers in one experiment of about 20 and in the other three of about 5 (i.e., K_T about 20 and 5 times molecular diffusion, respectively). **INDEX TERMS:** 4568 Oceanography: Physical: Turbulence, diffusion, and mixing processes; 4524 Oceanography: Physical: Fine structure and microstructure; 4219 Oceanography: General: Continental shelf processes; **KEYWORDS:** continental shelf, microstructure, mixing

Citation: Oakey, N. S., and B. J. W. Greenan (2004), Mixing in a coastal environment: 2. A view from microstructure measurements, *J. Geophys. Res.*, 109, C10014, doi:10.1029/2003JC002193.

1. Introduction

[2] The Coastal Mixing and Optics Experiment (CMO) was carried out on the New England continental shelf in 1996–1997 [Dickey and Williams, 2001]. The objective of this field program was to improve the understanding of vertical mixing processes on the continental shelf, and to determine the effect of mixing on the optical properties of the water column. Vertical mixing can have an impact in a variety of ways. Bottom boundary layer mixing influences sediment resuspension and transport, mixing in the water column affects particulate and dissolved matter distributions and concentrations, and vertical transport of nutrients plays an important role in plankton dynamics.

[3] As part of this experiment, measurements of dissipation of turbulent kinetic energy and dissipation of temperature variance were carried out by our research group to estimate diapycnal diffusivities. This type of measurement, the most prevalent method over the past 3 decades of estimating ocean mixing from field measurements, uses microstructure sensors to observe centimeter-scale fluctua-

tions in velocity and temperature fields. The use of injected tracers to estimate diapycnal diffusivities in the ocean has increased substantially over the last decade [Ledwell et al., 1998; Houghton and Ho, 2001]. Each of these methods has certain inherent advantages in estimating vertical mixing rates. Nevertheless, a comparison of the two methods on similar time and space scales has never been attempted. Therefore an integrated field program using injected dyes and a microstructure profiler was carried out during CMO. The results of the dye dispersion experiment are presented and discussed in a companion paper by *Ledwell et al.* [2004] (hereinafter referred to as LDSS). A detailed description of the site of the experiment and many of the operational details are described by LDSS, and will not be repeated here. In addition, LDSS provide a detailed comparison of the dye mixing results with dissipation-based measurements carried out by other researchers during CMO [MacKinnon and Gregg, 2003a, 2003b; Rehman and Duda, 2000; Duda and Rehman, 2002]. The objective of this paper is twofold. First, microstructure results will be compared with tracer measurements to determine how well the two methods agree in their estimates of mixing. Second, these results will be discussed in relation to the buoyancy frequency and gradient and flux Richardson numbers.

Table 1. Times and Depths of Experiments

| Experiment | Year | Date | Dye ^a | Target Depth, m | Bottom Depth, m | Target Density, kg/m ³ | Target N , cph | Dye Result | Microstructure Result |
|------------|------|-------------|------------------|-----------------|-----------------|-----------------------------------|------------------|------------|-----------------------|
| 1 | 1995 | 11–14 Sept. | Rhd | 40 | 70 | 25.20 | 13 | yes | no |
| 2 | 1996 | 6–10 Sept. | Rhd | 35 | 70 | 24.06 | 5.7 | no | yes |
| 3 | 1996 | 12–16 Sept. | Flr | 45 | 70 | 24.30 | 12 | yes | yes |
| 4 | 1997 | 1–6 Aug. | Rhd | 19 | 70 | 24.60 | 18 | yes | yes |
| 5 | 1997 | 7–12 Aug. | Flr | 65 | 70 | 26.14 | 20 | yes | yes |

^aRhd: rhodamine WT; Flr: fluorescein.

[4] The only field program prior to CMO to attempt an intercomparison of these two methods was the North Atlantic Tracer Release Experiment (NATRE). This experiment was carried out in the main pycnocline of the Atlantic in the Canary Basin over a period of 2 years (1992–1994) and showed that the two techniques yield similar estimates of vertical diffusivity, of order 2×10^{-5} m²/s [Ledwell *et al.*, 1998; Ruddick *et al.*, 1997]. However, in that study the microstructure estimates were obtained only during two sampling periods of 1 month, while the dye measurements represented the mixing averaged over 30 months. On the continental shelf we might expect mixing to be much larger than in the mid-ocean pycnocline, driven by stronger forcing at both the surface and bottom boundaries. Nevertheless, as we shall see, this was not the case for the studies reported here.

[5] The CMO study consisted of five separate experiments, a trial study in 1995 with no microstructure measurements (Experiment 1), two studies in September 1996, and two more in August 1997 with microstructure measurements (Experiments 2 to 5). These are summarized in Table 1. We have retained the names for the experiments used by Sundermeyer and Ledwell [2001] for consistency. The measurements for Experiments 2 to 5 were each done as follows. A tracer was injected on a target isopycnal surface, and the initial dye distribution was determined during a survey with a towed, undulating sled. Vertical profiles of temperature and velocity microstructure measurements were then obtained by sampling intensively using EPSONDE [Oakey, 1988] for a period of about a day. This was followed by re-surveying the dye distribution in the tracer patch to determine its dispersion. This alternate measurement of microstructure and dye dispersion was repeated 2 or 3 times until the tracer was quite dispersed. Each experiment took about 5 days.

[6] Vertical diffusivity estimated from the tracer is described in detail by LDSS. A summary is included here for completeness. For each sampling of the patch of dye, the vertical and horizontal distribution and concentration of tracer was determined by towing an instrumented measurement sled. The vertical distribution of tracer is obtained by averaging on isopycnal surfaces over the region encompassing the tracer patches. Repeated sampling of the tracer patch provides a time history of the vertical distribution of dye. From the broadening of this distribution in time the diapycnal mixing rate is determined. This time-integrated diapycnal mixing rate is compared to the microstructure measurements.

[7] Two traditional microstructure measurements, dissipation of turbulent kinetic energy and dissipation of temperature variance, have been used for many years to estimate diapycnal mixing rates applying a variety of

simplified model parameterizations. The theory behind these different models is well described in a number of papers [Oakey, 1982; Gregg, 1987; Ruddick *et al.*, 1997], and only the main equations will be presented here. These will be used as a basic comparison between diffusivities estimated from the tracer results and the microstructure profiles.

[8] The Osborn-Cox model [Osborn and Cox, 1972] assumes that temperature fluctuations are a result of turbulent overturns where a mean temperature gradient exists. Assuming stationarity, homogeneity, and a simplified form of the turbulent heat equation, the vertical diffusivity of heat may be expressed as

$$K_T = \frac{\chi}{2 \left[\frac{\partial T}{\partial z} \right]^2} \quad \text{m}^2/\text{s}, \quad (1)$$

where χ is the rate of diffusive smoothing of temperature fluctuations and is given by $\chi = 6\kappa_T(\partial T'/\partial z)^2$, where κ_T is the molecular diffusivity of heat. T denotes mean temperature, with T' used to designate temperature fluctuations; z is depth.

[9] The Osborn dissipation model [Osborn, 1980] uses a very simplified form of the turbulent kinetic energy equation and obtains a vertical diffusivity for density,

$$K_\rho \leq \Gamma \frac{\varepsilon}{N^2} \quad \text{m}^2/\text{s}. \quad (2)$$

Assuming isotropy, the rate of dissipation of turbulent kinetic energy is given by $\varepsilon = \frac{15}{2} \nu \left(\frac{du'}{dz} \right)^2$, where ν is the kinematic viscosity and u' is the turbulent velocity. N^2 ($\equiv -\frac{g}{\rho} \frac{\partial \rho}{\partial z}$) is the square of the buoyancy frequency. $\Gamma = R_f/(1 - R_f)$ is often referred to as the mixing efficiency, although this is a misnomer, since it is a ratio of the buoyancy flux to the dissipation and not a ratio of buoyancy flux to total energy input. The flux Richardson number, R_f , is defined by

$$R_f = \frac{J_b}{u'w'(\partial \bar{u}/\partial z)}. \quad (3)$$

This is the ratio of the production of buoyancy flux, J_b , to the production of turbulent kinetic energy, $u'w'(\partial \bar{u}/\partial z)$. The value of R_f is not well established. Osborn [1980] suggested a maximum value $R_{f\text{crit}} = 0.15$ based on a number of experiments and theoretical arguments. This is consistent with measured values of 0.21 [Oakey, 1985] and 0 to 0.2 for fluids with Prandtl numbers greater than 1 [Ivey and Imberger, 1991].

[10] The dissipation method [Gregg, 1987] leads to an eddy coefficient for momentum (the eddy viscosity), K_m .

$$K_m = \frac{\varepsilon}{(1 - R_f)[\partial\bar{u}/\partial z]^2} = \frac{R_i}{(1 - R_f)} \frac{\varepsilon}{N^2} \quad \text{m}^2/\text{s}. \quad (4)$$

This assumes that the momentum flux may be obtained from $\overline{u'w'} = -K_m \frac{\partial\bar{u}}{\partial z}$, where $\frac{\partial\bar{u}}{\partial z}$ is the mean shear. The gradient Richardson number is defined by

$$R_i = N^2 / [\partial\bar{u}/\partial z]^2. \quad (5)$$

2. EPSONDE Microstructure Profiler and Data Analysis

2.1. EPSONDE Microstructure Profiler

[11] Microstructure data were obtained using the EPSONDE profiler [Oakey, 1988]. This instrument is a vertical profiler, 2.4 m long with sensors on the leading end. The instrument was equipped with conventional CTD sensors to relate the microstructure observations to the larger-scale physical fields in which the measurements were made. The instrument uses a tether for rapid recovery and redeployment, and within the tether is a data link for telemetry of information from the instrument to shipboard logging computers. Data are recorded in compressed binary format for later analysis but are also analyzed in near real time for operator review to confirm that all sensors are working correctly. This is particularly important in experiments such as the CMO where profiling is done in coastal waters where the likelihood of damage to sensors by suspended material can be a particular problem. EPSONDE carries two sensors to measure temperature microstructure, a cold-film platinum thermometer with typical frequency response of 2 ms and a fast-tip thermistor with a frequency response of typically 12 ms. The fluctuations in temperature sensed from these two are sampled at 256 Hz and 128 Hz, respectively. The two sensors provide the advantage of redundancy. The faster cold film sensor will measure more of the temperature variance for high turbulence but with poorer signal-to-noise ratio. The thermistor measures temperature variance from lower turbulence levels with higher signal-to-noise ratio but with less frequency response. As noted later, the thermistor data are not used in the analysis, because of inadequate spatial resolution, even for the low levels of turbulence observed. However, they have been very useful in data quality control. The turbulent velocity signal was measured by two airfoil shear probes [Osborn and Crawford, 1980], which were aligned parallel to one another to provide redundant measures of the velocity gradient signal. These sensors were also sampled at 256 Hz. The instrument had its ballast adjusted to fall typically at 0.8 m/s.

2.2. CMO Sampling

[12] Normally, EPSONDE sampling would be done to the bottom or close to the bottom on the shelf with a guard ring at the leading end of the profiler that allows the instrument to land on the bottom. The sensors are behind the leading edge of the guard ring and come within less than 10 cm from the bottom. In the CMO area, there was a lot of debris on the bottom from both derelict and active fishing gear,

which made this mode of operation treacherous. As a compromise, sites were chosen which were believed to be relatively free of fishing gear. These sites were typically an east-west line of about 4 km in length. A Seabird 911plus CTD profile was taken by Ledwell's group at the start of the line. As the ship steamed the length of the line at a typical speed of 1 to 2 knots (less than 1 m s⁻¹), EPSONDE was dropped from the stern to within about 5 m of the bottom to avoid snagging any fishing gear. At the end of the line, another CTD profile was taken. Thus in one line transit, typically 25 microstructure profiles were obtained depending on the speed of the ship. This group of data was called a station. Upon completion of the station, the ship returned to the starting point of the line and the procedure was repeated. This procedure continued for approximately 24 hours between the dye surveys enabling us to complete about 10 stations at each line. This continuous sampling of a site over 1 day reduces potential sampling problems related to internal tides. By making measurements over a day, we sample mixing rates representative of a complete tidal cycle. If mixing rates are related to tidal shears, this is a suitable sampling period. Shorter internal wave variability is averaged out by the large number of samples every hour.

2.3. Data Analysis

[13] Data from the EPSONDE profiles were analyzed in segments of 2 s that corresponded to about 1.6 m vertically. Microstructure data from the temperature and velocity shear sensors were analyzed using standard FFT and spectral analysis techniques to obtain the variance associated with the turbulent fluctuations using information about universal turbulence spectra to discriminate against instrument noise. Because of the drop speed of the instrument (typically 0.8 m/s) and the sampling frequency (256 Hz), the spectra of turbulent shear were well resolved. To resolve all of the variance in the velocity shear spectrum, one must be able to measure at least to the frequency defined by the Kolmogorov wave number ($k_K = (\varepsilon/\nu^3)^{0.25}$ rad/m), where viscosity defines the size of the smallest eddy. At a drop speed of 0.8 m/s a sampling frequency of 256 Hz resolves all of the dissipation up to 10⁻⁵ W/kg, substantially higher than found in this study. The dissipations ε_1 and ε_2 were calculated for each of the shear probe sensors, and the average shear variance was used to compute the dissipation, ε . For temperature microstructure the spectral cutoff frequency extends to about 3 times that defined by the Kolmogorov wave number (the Batchelor cutoff wave number $k_B = (\varepsilon/\nu\kappa_T^2)^{0.25}$). This frequency may not be fully resolved either because of high dissipation or instrument noise. By experience, we believe that the Batchelor universal spectral form (described by Oakey [1982]) is a good approximation to the high-frequency part of the temperature gradient spectrum. Since in this study we resolve the entire dissipation spectrum, we can use the Batchelor spectrum to readily compute the percentage of the temperature microstructure spectrum that has been measured. This is done by computing the cutoff frequency corresponding to the Batchelor wave number, comparing it to the highest measured spectral frequency, computing the lost variance from the universal Batchelor spectrum and then correcting measured temperature variance for lost variance. For the cold-film thermometer, more than 80% of the time, greater than 75%

of the temperature variance was measured, and 99% of the time, more than 50% of the variance was measured, with no cases where <40% of the variance was determined. Here χ , as used in equation (1), was then calculated using $\chi = 6\kappa_T(\partial T'/\partial z)^2$. The thermistor data were not used to calculate χ in the current paper because although the two temperature sensors agreed at lower dissipation levels, at higher levels ($\varepsilon > 1.0 \times 10^{-7}$), too large a correction had to be applied to the thermistor variance because of inadequate spatial resolution.

[14] In an editing process, the four spectra from cold-film thermometer, thermistor, and two shear probes were viewed for each segment along with appropriate diagnostic information to determine whether the data were self consistent. Clearly bad data segments were rejected at this time. The remaining good microstructure data ($\chi_{\text{Thin-Film}}$, ε_1 , and ε_2) were archived in a database along with EPSONDE CTD data.

[15] To determine vertical diffusivity to compare with the dye measurements, the database was searched to find values of microstructure quantities that corresponded to density ranges bracketing the isopycnal on which the tracer was injected. In each microstructure profile, values of $\chi_{\text{Thin-Film}}$, ε_1 , and ε_2 between density limits were selected that satisfied the following criteria: (1) all three microstructure values were good, (2) temperature and density gradients were above the instrument noise level, (3) EPSONDE was falling freely and at the correct speed, and (4) corrections applied to $\chi_{\text{Thin-Film}}$ were acceptably small. Some profiles were excluded from the search (about 50 out of more than 1500) in which there was poor T-S data resulting from bad salinity measurements which we attribute to the cell capturing a contaminant during its profile. Finally, there were a few (order 10) segments which gave outliers as much as 3 orders of magnitude from the mean, and these were examined carefully and in most cases eliminated for a variety of objective reasons. The remaining good 1.6-m segments of microstructure data at the target surface form the basis for the comparison with the tracer.

2.4. Averaging Technique Used to Determine Diffusivity

[16] Each of the vertical diffusivities K_T , K_p , or K_m (equations (1), (2), and (4), respectively) involve the ratio of a microstructure variance and a mean quantity. The theories used to derive the diffusivities are based on assumptions of isotropy, homogeneity, and stationarity. This allows one to ignore all of the terms in the turbulent kinetic energy equation or the turbulent heat equation except the production and dissipation terms, which are considered in balance. These assumptions are often difficult to justify [Davis, 1994, 1996; Sherman and Davis, 1995; Yamazaki and Osborn, 1990]. Every good segment of data (designated by the subscript i) generated values of ε_i , χ_i , N_i , T_{zi} , or other mixing quantity in a selected density interval. These data represent a complicated set of independent measures of these quantities in a station with a spatial scale of about 4 km and a temporal scale of 2 to 3 hours. To form the average representing a density interval for this station, we average the values as follows to estimate diffusivity, $K_{j\text{stn}}$. For example $\varepsilon_{j\text{stn}} =$

$\langle \varepsilon_i \rangle_{\text{stn}}$, $N_{j\text{stn}}^2 = \langle N_i^2 \rangle_{\text{stn}}$, and $K_{j\text{stn}} = \Gamma(\varepsilon_{j\text{stn}}/N_{j\text{stn}}^2)$. The estimate of the diffusivity for the experiment is then given by the average $K_p = \langle K_{j\text{stn}} \rangle$. We form the averages for the other diffusivities, K_T in a similar way. In this notation, $\langle \rangle_{\text{stn}}$ is an average over all i segments in a station in a particular density interval.

[17] The calculation of K_m was somewhat more complicated. K_m (equation (4)) and R_i (equation (5)) were calculated by using the velocities measured from the shipboard ADCP in conjunction with the density information from the EPSONDE microstructure profiler. Each ADCP velocity profile was derived using a vertical bin size of 2 m and time averaging of 3 min. The data sets from the ADCP and microstructure measurements were merged. The ADCP bin was paired with the segment in the EPSONDE database that most closely matched in both depth and time. The vertical shear was calculated from differences in the velocities in the ADCP bin above and below. It thus represents a shear over a distance of 4 m. In this case, the averages for the station were obtained by calculating $N_{j\text{stn}}^2 = \langle N_i^2 \rangle_{\text{stn}}$, $\varepsilon_{j\text{stn}} = \langle \varepsilon_i \rangle_{\text{stn}}$, $u_z^2{}_{j\text{stn}} = \langle (\partial \bar{u} / \partial z)_i^2 \rangle_{\text{stn}}$, $R_{i\text{stn}} = (N_{j\text{stn}}^2 / u_z^2{}_{j\text{stn}})$, and $K_{M\text{stn}} = (1/1 - R_f)(\varepsilon_{j\text{stn}} / u_z^2{}_{j\text{stn}})$ for each station and then averaging for all the stations, $R_i = \langle R_{i\text{stn}} \rangle$ and $K_M = \langle K_{M\text{stn}} \rangle$.

3. Estimation of Vertical Mixing Rates From Microstructure

3.1. Experiment 3

[18] The first experiment to review in detail is the second dye injection of the 1996 field program, which is identified as Experiment 3 (see Table 1). An overview of this experiment is shown in Figure 1. Injection of fluorescein dye was done at about 45 m at a density level of $\sigma_\theta = 24.30$ just east of the along-shore (eastern) mooring on day of year (DOY: 1 January = day 1) 256.2, 1996. The mid-times of three surveys of the diapycnal and horizontal evolution of the tracer were on DOY 256.7, 258.5, and 260.5. The shaded area surrounding the center at the filled triangle indicates the 4σ extent of the tracer patch [Sundermeyer and Ledwell, 2001]. The line connecting the centers of each dye survey indicates the mean water trajectory as calculated using the ADCP water velocity at the depth of the tracer. Three sets of EPSONDE microstructure profiles were interspersed with the tracer measurements. The first was done on DOY 257.5 just north and east of the central mooring after the first dye survey with a very good overlap between dye path and microstructure. A second set of EPSONDE profiles was obtained on DOY 259.5 after the second dye survey at a site to the north and west of the central mooring with a good overlap with dye as it moved west. The third EPSONDE survey on DOY 261.3 was completed following the third dye survey at a westerly third site near 71°W to overlap with the tracer. It would have been ideal to do EPSONDE profiles at exactly the same place as the dye patch evolved. Nevertheless, fishing gear in the area prevented this and limited profiles to be no closer than 5 m from the seabed. Therefore lines were chosen that were clear of fishing gear and "reasonably close" to the expected dye trajectory. From injection to the site of the final survey, the dye moved about 55 km along the shelf in about 5 days. There was an excellent overlap in space and time between the measurements by two techniques with approximately

1996: Experiment 3

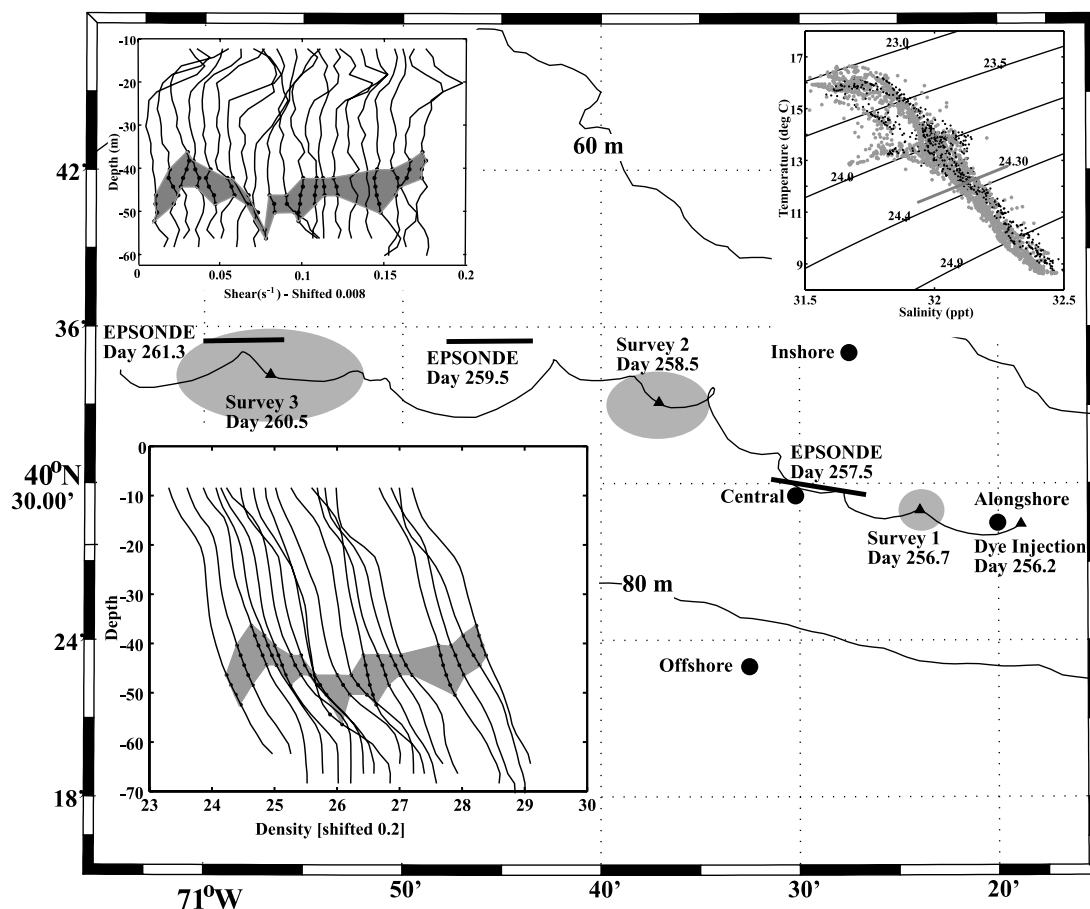


Figure 1. Summary of Experiment 3 (1996: dye release 2, fluorescein). The dye experiment included the dye injection and three surveys (triangles). Three sets of microstructure data were collected along three lines. The solid line indicates the path of the center of the tracer patch projected between the surveys using hourly ADCP velocities. This line extends beyond survey 3 to the time of the last EPSONDE survey. Shaded ellipses indicate the 4σ extent of the tracer patch in the zonal and meridional directions [Sundermeyer and Ledwell, 2001]. The CMO mooring sites are indicated by the solid circles. The inset at the bottom left shows successive average density profiles for the EPSONDE stations obtained for the microstructure survey. Successive profiles are offset by 0.2. The shaded area represents the range of σ_θ from 24.15 to 24.45 kg m^{-3} centered on the target isopycnal at 24.3 kg m^{-3} . At the top right, a composite TS plot is shown for the experiment. Shaded dots are from EPSONDE, and black dots are from the CTD profiles taken at the beginning or end of each EPSONDE line. The top left inset shows a waterfall plot of the shear from the shipboard ADCP. Each profile is the average over one EPSONDE station. Successive profiles have been offset by 0.008. The shaded region corresponds to the range of σ_θ from 24.15 to 24.45 kg/m^3 centered on the target isopycnal at 24.3 kg/m^3 .

525 microstructure-mixing profiles obtained during 56 hours of sampling.

[19] Mean density profiles for each EPSONDE station for Experiment 3 are shown in the inset at the bottom left of Figure 1. Each profile is the average of typically 25 EPSONDE profiles obtained in a station that we define as one occupation of a survey line. The inset includes data from all three surveys. The shaded area represents the range of σ_θ from 24.15 to 24.45 kg m^{-3} centered on the target isopycnal at 24.3 kg m^{-3} . In this interval $N = 10.0$ cph at a mean depth of about 45 m. The shaded area typically represents 3 or 4 microstructure segments (of 1.6 m).

Because of the variability of isopycnal depth with time, it was necessary when selecting the EPSONDE data points to scan the database with a density criterion rather than just using depth. The TS plot for this experiment is shown in the inset at the top right of Figure 1. EPSONDE CTD data (shaded dots) were corrected to match the Sea-Bird CTD data (a correction of -0.050 kg m^{-3}). There is good agreement between the EPSONDE and Sea-Bird CTD at the level of the dye injection. This assured that when the microstructure data were searched on density, the mixing results corresponded to the injection density surface of 24.3 kg m^{-3} . A waterfall plot of the vertical shear for

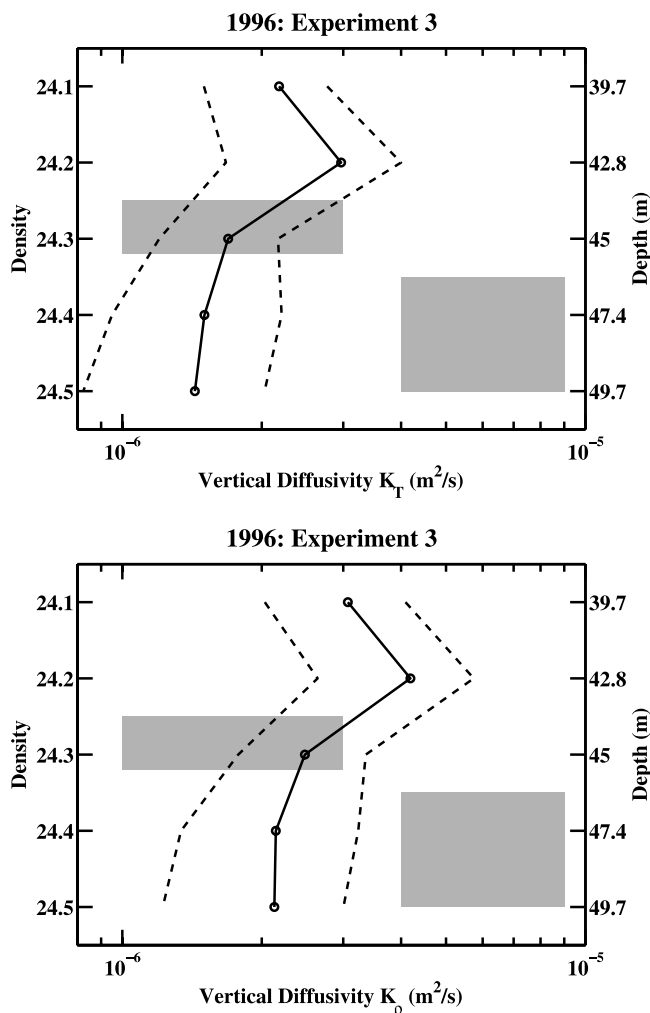


Figure 2. (top) Profile of the vertical diffusivity K_T near the density of the target isopycnal for Experiment 3 (in this case at $\sigma_\theta = 24.3$ near 45 m). The diffusivity is shown as a solid line with the center of each density bin marked by a circle. The 95% confidence intervals of the mean estimated using a bootstrap technique are shown as dashed lines. (bottom) Similar information for the vertical diffusivity K_ρ . For these estimates, the mixing efficiency used was arbitrarily chosen as $\Gamma = 0.25$. The range of diffusivity and the depth range over which it applies, obtained from the tracer, is shown by the shaded bars for the region above and below the target isopycnal.

Experiment 3 is shown in the inset at the top left of Figure 1. Each profile is the average over one EPSONDE station. Again, the shaded region represents the range of σ_θ from 24.15 to 24.45 kg m^{-3} centered on the target isopycnal

at 24.3 kg m^{-3} . These data were obtained from the shipboard ADCP and will be merged in calculations presented later to calculate vertical diffusivities of momentum, K_m (equation (4)).

[20] A comparison of the mixing rates from the dye and microstructure is shown in Figure 2 and Table 2 for the two measures of vertical diffusivity estimated directly by EPSONDE. The top panel of Figure 2 shows K_T (equation (1)) for five density intervals between 24.05 and 24.55 kg m^{-3} centered about the injection surface of 24.3 kg m^{-3} . The 95% confidence intervals are estimated using a bootstrap technique and shown as dashed lines. The shaded areas represent the limits of the diffusivity estimated from fluorescein dye dispersion (LDSS). The dye mixed vertically at different rates above and below the level of the injection and, therefore, LDSS provide two estimates of diffusivity for this experiment. The increased mixing below the injection was not observed in the microstructure data.

[21] In the bottom panel of Figure 2, K_ρ (from equation (2)) is plotted. In our calculations the value of the mixing efficiency Γ was arbitrarily chosen to be 0.25, a value commonly used [Oakley, 1982] but too large in this case, since the calculated K_ρ is greater than K_T .

[22] For Experiment 3, a larger portion of the profile was examined to determine the variability in vertical diffusivity, K_T , from well above to well below the target isopycnal. Figure 3 shows a plot of K_T over the range of σ_θ from 23.4 to 25.2 kg m^{-3} where the target isopycnal is at 24.3 kg m^{-3} . This corresponds to the depth from about 15 m to deeper than 55 m, with the target isopycnal at 45 m. (This upper limit is well below the depth of 5 m from the surface where the data may be contaminated by the ship's wake.) Very low vertical diffusivities persisted throughout the water column, never exceeding $10^{-5} \text{ m}^2 \text{ s}^{-1}$ even nearer the surface and only about $2 \times 10^{-6} \text{ m}^2 \text{ s}^{-1}$ at the depth of the dye. Only in Experiment 5 within 3 m of the bottom were larger diffusivities observed.

3.2. Experiment 4

[23] The first dye injection of 1997 (Table 1) is described in Figure 4 in a format similar to Figure 2. Injection of Rhodamine dye was done at about 19 m at a density level of $\sigma_\theta = 24.60$ just south of the along-shore (eastern) mooring on DOY 213.7, 1997. Three surveys of the diapycnal and horizontal evolution of the tracer were done on DOY 214.1, 215.8, and 218.1. Three EPSONDE surveys were interspersed with the tracer measurements along a 6-km line just south of the mooring, since there was little along-shelf advection of the tracer. During this dye experiment we profiled only to within about 5 m of the bottom because of concerns of instrument safety. Microstructure measurements were done prior to injection on DOY 213.1 and after the

Table 2. Comparison of Diffusivities for Dye and Microstructure

| Experiment | Mean Depth, m | Condition | Mean Density | Mean N , cph | $K_{\text{dye}} \times 10^{-6} \text{ m}^2/\text{s}$ | Microstructure $K_T \times 10^{-6} \text{ m}^2/\text{s}$ |
|------------|---------------|--------------|--------------|----------------|--|--|
| 2 | 30.5 | | 24.03–24.09 | 6.2 | <30 | 5.7–14.7 |
| 3 | 45 | target | 24.25–24.35 | 10.0 | 1–3 | 1.2–2.2 |
| 3 | 47.4 | below target | 24.35–24.45 | 11.9 | 4–9 | 1.0–2.2 |
| 4 | 17 | | 24.52–24.72 | 16.9 | 1.4–2.2 | 1.0–2.0 |
| 5 | 62.2 | above target | 25.99–26.09 | 13.5 | 0–2.4 | 2.0–2.8 |
| 5 | 64.8 | below target | 26.19–26.29 | 18.8 | 0.7–2.1 | 1.9–3.3 |

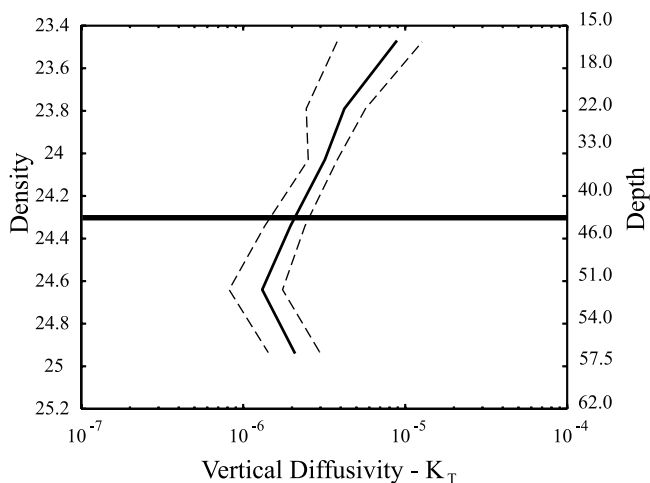


Figure 3. Plot of extended profile of vertical diffusivity, K_T , versus density for Experiment 3. The dashed lines delimit the 95% confidence interval of the mean. The horizontal line represents the density of the target isopycnal. The corresponding depths are shown on the right. Diffusivity has been averaged in density bins of 0.3 kg m^{-3} . Microstructure data were measured from about 5 m below the surface (above which one might expect the ship's wake to be a problem) to near the bottom. Only the extended profile, in the region of interest from well above to well below the target isopycnal, is shown.

first and second dye surveys on DOY 214.9 and 216.8. The lack of advection in this experiment provided excellent overlap in space and time between the dye and microstructure surveys with over 700 microstructure profiles in 74 hours of sampling.

[24] Mean density profiles for each EPSONDE station (the average of all profiles in one occupation of a survey line) are shown in the lower left inset. The format is identical to Figure 1 except that in this case the shaded area represents the range of σ_θ from 24.3 to 24.9 kg m^{-3} centered on the target isopycnal at 24.6 kg m^{-3} . In this interval, $N = 16.9$ cph at a mean depth of about 17 m. The shaded area typically represents three or four microstructure segments (of 1.6 m). The TS plot is shown in the bottom right of Figure 4. EPSONDE CTD data (shaded dots) were corrected to match the Sea-Bird CTD data (a correction of -0.020 kg m^{-3}).

[25] A comparison of the mixing rates from the dye and microstructure is shown in Figure 5 and Table 2 for Experiment 4. The diffusivity K_T is plotted for five density intervals between 24.10 and 25.10 kg m^{-3} centered about the injection surface of 24.6 kg m^{-3} . Confidence intervals are determined by a bootstrap method. The shaded area represents the upper and lower bounds of the diffusivity estimated from Rhodamine dye dispersion (LDSS). The error bounds on the microstructure data are significantly smaller than in Experiment 3, which seems consistent with the narrower range of diffusivity estimated from the dye measurements. Estimates of K_ρ are not shown for this experiment but give similar results to Experiment 3 with K_ρ larger than K_T . The close overlap in time and space of this experiment means that there were fewer complicating factors, and

that we might expect better agreement between the two methods.

3.3. Experiment 5

[26] Experiment 5 was the second dye injection of 1997 (summarized in Figure 6 and Table 1). Injection of fluorescein dye was done at a depth of about 65 m (about 5 m above bottom) at a density level of $\sigma_\theta = 26.14$ on DOY 219.7, 1997. This was followed by a dye survey to the southeast of the injection site on DOY 220.1. On DOY 220.9, an EPSONDE survey was done close to the injection site along a 5-km line which was about 1 km to the south of the central mooring. In this experiment, a concerted effort was made to profile right to the bottom. Nevertheless, with a ship speed of about 1.5 to 2 knots and the instrument drop speed of 0.8 m/s, no more than 70% of the profiles reached the bottom. Significantly, more were within a couple of meters of the bottom. Sensors were protected by a landing guard allowing microstructure to be measured to within about 10 cm of the bottom. The horizontal dispersion of the tracer patch is not shown in this case (see LDSS), although the solid line obtained from the ADCP data indicated the evolution of the center of the dye patch. Because the dye patch had moved significantly to the east, the second (and final) EPSONDE survey was done on DOY 223.2 at the site previously surveyed in Experiment 4 just south of the along-shore mooring. The final dye survey continued significantly to the east on DOY 224.3. This experiment had reasonably good overlap between tracer and microstructure. As the dye moved to the east, and particularly between dye surveys 2 and 3, a wedge of warmer, saltier water moving up the shelf intruded under the patch of dye close to the bottom. This complicates the comparison between the microstructure and dye in this final experiment, although EPSONDE surveys 1 and 2 overlap well with dye surveys 1 and 2, with nearly 400 microstructure profiles in 53 hours.

[27] Mean density profiles for each EPSONDE station (~ 25 instrument drops) for Experiment 5 are shown in the inset at the bottom left of Figure 6. The format is identical to Figure 1 except that in this case the shaded area represents the range of σ_θ from 25.89 to 26.39 kg m^{-3} centered on the target isopycnal at 26.14 kg m^{-3} . In this interval, $N = 16.1$ cph at a mean depth of about 65 m. The shaded area typically represents 3 or 4 microstructure segments (of 1.6 m). The TS plot is shown at the bottom right of Figure 6, as in Figure 4. EPSONDE CTD data (shaded dots) were corrected to match the Sea-Bird CTD data (a correction of -0.020 kg m^{-3}). There are TS differences between the first and second survey higher in the water column, but these are not evident deeper where the dye was injected.

[28] A comparison of the mixing rates from the dye and from the microstructure is shown in Figure 7 and Table 2 as in the previous two experiments. K_T is plotted for five density intervals between 25.79 and 26.39 kg m^{-3} centered about the injection surface of 26.14 kg m^{-3} . In this experiment, much of the dye remained off the bottom and was swept eastward, while a smaller fraction mixed downward into an onshore flow (Figures 15 and 17 of LDSS). As with Experiment 3, diffusivity estimates from the dye increase with depth as N increases. For this experiment, LDSS only estimate an upper bound of 2.4×10^{-6} for the upper part of the patch as indicated by the arrow in Figure 7.

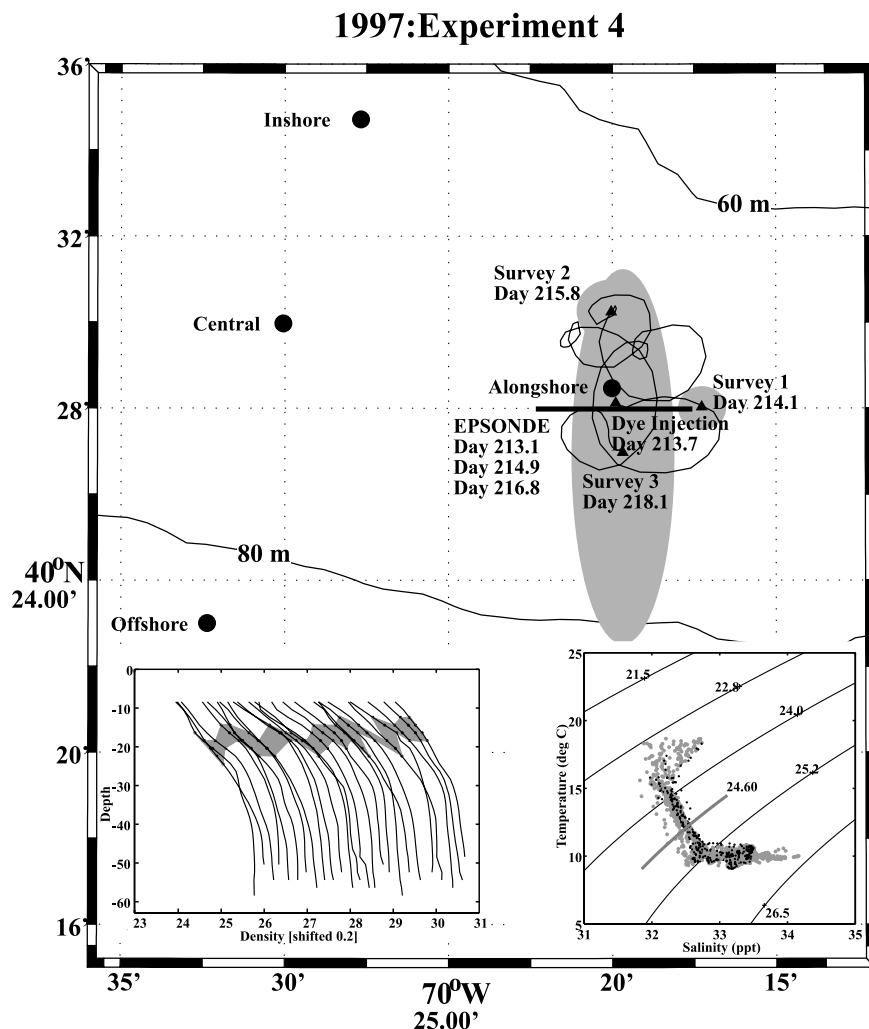


Figure 4. Location of events for Experiment 4 (1997: dye release 1, Rhodamine). Notation is similar to Figure 1. This experiment included the dye injection and three surveys (triangles). Three sets of microstructure data were collected along one line. The solid line indicates the path of the center of the tracer patch projected between the surveys using hourly ADCP velocities. Shaded ellipses indicate the 4σ extent of the tracer patch in the zonal and meridional directions [Sundermeyer and Ledwell, 2001]. The inset at bottom left shows successive average density profiles for the EPSONDE stations obtained for the microstructure survey. The shaded area represents the range of σ_θ from 24.3 to 24.9 kg/m^3 centered on the target isopycnal at 24.6 kg/m^3 . A composite TS plot is shown at the bottom right. Shaded dots are from EPSONDE, and black dots form the CTD profiles taken at the beginning or end of each EPSONDE line. At the depth of the dye injection at $\sigma_\theta = 24.6$, there is good agreement between the EPSONDE and CTD density calculations.

A dye value of $0.7\text{--}2.1 \times 10^{-6}$ W/kg is estimated for the lower part of the patch. Both are in moderate agreement with the microstructure measurements.

3.4. Experiment 2

[29] A summary of the first experiment in 1996, experiment 2, is shown in Figure 8. Injection of Rhodamine dye was done at about 32 m at a density level of $\sigma_\theta = 24.06$ just south of the along-shore (eastern) mooring on DOY 250.9, 1996. The mid-times of three surveys of the diapycnal and horizontal evolution of the tracer were on DOY 251.5, 252.8, and 254.1. On DOY 250.1, a preliminary EPSONDE survey was done northeast of the central mooring prior to

dye injection. Instrument problems prevented microstructure studies after the first dye survey, so the second microstructure study was done on DOY 253.4 following the end of the second dye survey. A final series of microstructure profiles was done on DOY 255.0 just after the third dye survey at a site northwest of the central mooring because the dye had moved significantly west. In the 4 days from injection to the final survey, the dye moved about 35 km along the shelf. The dye trajectory passed through both EPSONDE study lines. We obtained more than 400 microstructure-mixing estimates during 44 hours of vertical profiling. Although not exactly co-located in space and time with the patch of dye, these

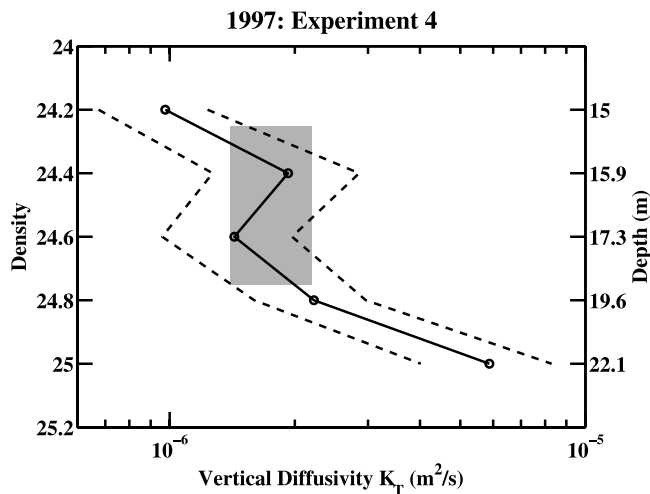


Figure 5. Vertical profile of the vertical diffusivity K_T is shown in the vicinity of the target isopycnal for Experiment 4 (in this case at $\sigma_\theta = 24.6$ near 17 m). The diffusivity is shown as a solid line with the center of the density bin indicated by a circle. The 95% confidence intervals of the mean estimated using a bootstrap technique are shown as dashed lines. The estimated value obtained from the tracer is shown by the shaded bar which indicates the density range as well as the range of diffusivity.

estimates were clearly representative of the path that the dye followed.

[30] Mean density profiles for each EPSONDE station (~ 25 instrument drops) are shown in the bottom left inset of Figure 8. The shaded portion of the waterfall plot indicates the depth variability of the isopycnals centered on the dye injection surface at 24.06 kg m^{-3} . The upper and lower limits of the shaded region are, respectively, 23.97 and 24.15 kg m^{-3} . The gap in the center of the data is a result of instrument problems. The TS plot is shown in the top right inset of Figure 8. The injection density of the dye (24.06 kg m^{-3}) is indicated. EPSONDE CTD data after the instrument problems have been corrected to match the Sea-Bird CTD data (a correction of -0.025 kg m^{-3}). This figure shows clearly that both the dye and microstructure parts of the experiment are using the same density reference. The density field changed between the beginning and end of the experiment. The mean density gradient at the end is less than at the beginning, and the TS curve indicates that the water is saltier and warmer at the end than at the beginning.

[31] The microstructure estimates of K_T for Experiment 2 are shown in Figure 9 and Table 2. LDSS had difficulties in making an estimate of diffusivity for this dye release because of poor separation of the dye signal from the background fluorescence in this experiment. Hence they were only able to estimate an upper limit of $3 \times 10^{-5} \text{ m}^2/\text{s}$ to compare with the microstructure. In this experiment the vertical diffusivities at the level of the dye injection are nearly an order of magnitude larger than those measured in Experiments 3, 4, and 5. The primary difference in this case

is the lower stratification of 6.2 cph after the passage of Hurricane Edouard.

4. Comparison With Dye-Based Measurements

4.1. Experiment 3

[32] The vertical diffusivity from the microstructure measurements is compared to the dye measurements in Figure 2. The top and bottom panels show the vertical diffusivity determined from the temperature microstructure (K_T) and velocity microstructure (K_p), respectively. Since the determination of K_p requires a mixing efficiency Γ , we have used an accepted value [Oakey, 1982] for this parameter of $\Gamma = 0.25$. Alternatively, one can assume that the diffusivities for heat and density are the same and use the measurements to determine a value of Γ or more correctly of flux Richardson number, R_f . This will be the approach in this paper. Overlaid on the EPSONDE diffusivity are values from dye measurements (LDSS). The dye results indicated an asymmetry in the distribution of tracer with an excess below the target isopycnal compared to above. In the advective-diffusive model used by LDSS to determine the diffusivity, this suggested an increase from order $1-3 \times 10^{-6} \text{ m}^2 \text{ s}^{-1}$ above the target surface to $4-9 \times 10^{-6} \text{ m}^2 \text{ s}^{-1}$ below. The corresponding values for the microstructure (Table 2) are $1.2-2.2 \times 10^{-6} \text{ m}^2 \text{ s}^{-1}$ and $1.0-2.2 \times 10^{-6} \text{ m}^2 \text{ s}^{-1}$. The microstructure and dye results are in good agreement near the target surface, but the larger diffusivity below the target surface indicated by the dye is inconsistent with the microstructure measurement. The mixing rate from microstructure measurements is examined over a much wider depth range in Figure 3. This gives no indication that there is any measurement of diffusivity from microstructure in this experiment as large as estimated by the dye measurements just below the target density surface.

[33] In August 1996, MacKinnon and Gregg [2003a, 2003b] found that solitary wave packets passed through the CMO site at most once per tidal cycle. Nevertheless, they found that these packets contributed significantly to mixing during this period. They were described as solibores that are waves that can have properties anywhere between the extremes of a soliton and a pure internal bore. They identified large increases in the depth averaged baroclinic energy [MacKinnon and Gregg, 2003a, Figure 4] at solibore times. In the first few days of September, the passing of Hurricane Edouard significantly reduced the stratification in this area [Lentz *et al.*, 2003]. Prior to this event, a 10-m-deep mixed surface layer existed over a stratified interior, providing an environment that supported the generation of solitary wave packets on the continental shelf. The greatly reduced stratification after Edouard and the lack of a well-defined mixed layer with the associated strong density gradient below would mitigate solitary wave packets at the CMO site. To determine whether solibores might be influencing our mixing results, time series of the barotropic and depth-averaged baroclinic energy (Figure 10) were derived using shipboard ADCP measurements. The high-energy, short timescale baroclinic events that were observed by MacKinnon and Gregg [2003a] during their cruise in August are not evident in the ADCP time series from September. The total energy of the events which MacKinnon and Gregg [2003a] attributed to passing solitary waves had values as large as 0.1 J kg^{-1} ,

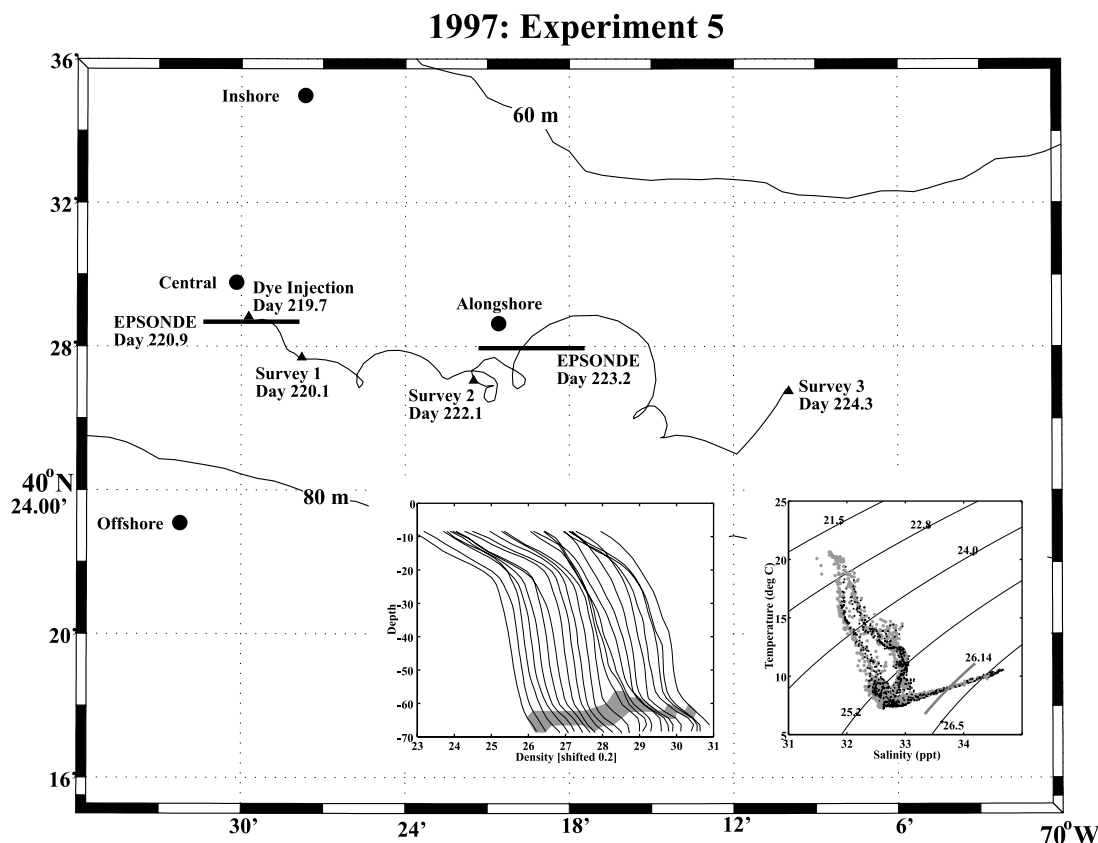


Figure 6. Similar to Figure 1, the events for CMO Experiment 5 (1997: dye release 2, fluorescein) are shown. The experiment included the dye injection and three surveys (triangles). Two sets of microstructure data were collected along two lines. The solid line indicates the path of the center of the tracer patch projected between the surveys using hourly ADCP velocities. Successive average density profiles are shown in the inset at bottom left for the EPSONDE stations. The shaded area represents the range of σ_θ from 25.89 to 26.39 kg/m^3 centered on the target isopycnal at 26.14 kg/m^3 . A composite TS plot is shown in the other inset. Shaded dots are from EPSONDE, and black dots from the CTD profiles taken at the beginning or end of each EPSONDE line.

which is an order of magnitude larger than the energy levels observed during our cruise. The peak baroclinic energy before the passage of Edouard was similar to the energy levels in the barotropic mode, but during our experiment it is at least an order of magnitude lower.

[34] One might also ask whether, at the low mixing rates observed, the towed dye measuring sled or the EPSONDE profiler could cause any appreciable mixing. A simple calculation of the rate at which work is done as the instruments profile, divided by the volume of the dye patch, gives an estimate equivalent to dissipation (W/kg). Using equation (2) with typical values of N^2 suggests that the largest mixing caused by the dye tow sled would be about 2 orders of magnitude less than that observed. An equivalent calculation for EPSONDE indicates that its influence would be 4 orders of magnitude lower.

[35] LDSS have explored the occasional occurrence of regions of high shear in an attempt to explain the difference between microstructure and dye results. In their Figure 21, an event in the ADCP record was observed to occur near the time when a CTD measurement was being done at the interval between EPSONDE stations. Although subsequent EPSONDE profiles indicated somewhat elevated dissipation

measurements (which were included in the microstructure averages), the event was poorly sampled with the microstructure profiler. It is tantalizing although speculative that occasional short-term (much less than an hour) events may explain the differences between the dye and microstructure measurements. It is still fair to say that the discrepancy between dye and microstructure in Experiment 3 is, at this point, unexplained.

4.2. Experiment 4

[36] The comparison between dye and microstructure diffusivities for Experiment 4 is shown in Figure 5, and details are listed in Table 2. This experiment, done in August 1997 at a depth of about 17 m was characterized by a moderate stratification ($N = 17$ cph) following a storm about 10 days prior to the experiment [see *Ledwell et al.*, 2004, Figure 10]. There was little wind stress during the study, so, although the target isopycnal was quite near the surface, there was little mixing from surface forcing. The diffusivity for the dye was $1.4\text{--}2.2 \times 10^{-6} \text{ m}^2 \text{ s}^{-1}$, in good agreement with K_T of $1.0\text{--}2.0 \times 10^{-6} \text{ m}^2 \text{ s}^{-1}$ estimated from the microstructure at the target surface. There is an indication of an increase in diffusivity with

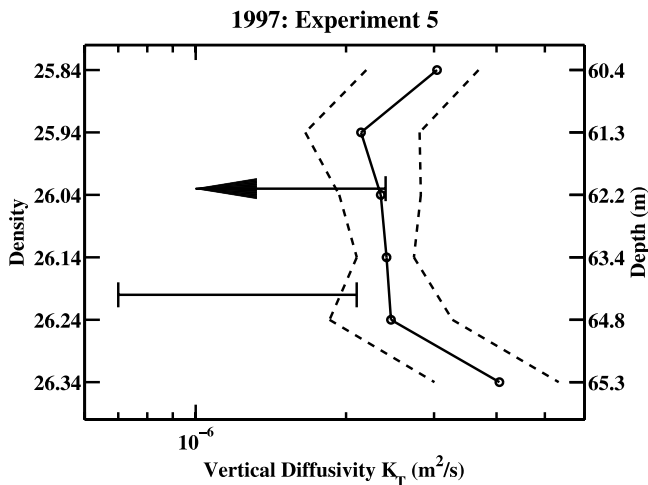


Figure 7. A vertical profile of the vertical diffusivity K_T is shown at a density near the target isopycnal for Experiment 5 (in this case at $\sigma_\theta = 26.14$ near 63 m deep). The notation is the same as for Experiment 4, Figure 5. Two regions of mixing were evaluated in the dye study. Above the target isopycnal the mixing rate was estimated to be less than $2.4 \times 10^{-6} \text{ m}^2/\text{s}$, indicated by the left pointing arrow. Below the target isopycnal the mixing rate was estimated to be $0.7\text{--}2.1 \times 10^{-6} \text{ m}^2/\text{s}$ as indicated by the lower range bar.

depth. This suggests that mixing is not from the surface forcing, but from sources within the water column such as internal waves or from tidal energy and shear in the water column. The ADCP energy time series from August 1997 (Figure 11) does show some evidence of short-term events that might be attributable to solitary wave packets. However, the energy levels are much lower than those observed by *MacKinnon and Gregg* [2003a] in August of the previous year. In comparison to 1996 (Figure 10), Figure 11 indicates lower energy levels in the barotropic tidal energy and similar levels in the depth-averaged baroclinic energy. Most of the short-term events in the baroclinic depth-averaged energy of Figure 11 are strongest in the upper 22 m (not shown) in the region where the density gradient is the greatest (inset Figure 4). Since this is the location of the dye, this energy is likely the source of mixing.

4.3. Experiment 5

[37] The agreement between mixing rates for Experiment 5 for dye and microstructure is summarized in Figure 7. This experiment was complicated because the upper part of the dye patch moved along-shore to the east and a wedge of warmer, saltier water intruded along the bottom, taking the lower part of the dye patch with it. It appeared from the TS plots (bottom right inset, Figure 6) that most of the separation at the bottom boundary occurred after the second EPSONDE microstructure survey, with good overlap between the dye and microstructure measurements to that time. Our microstructure measurements indicate a nearly constant diffusivity above the target isopycnal where K_T was $2.0\text{--}2.8 \times 10^{-6} \text{ m}^2 \text{ s}^{-1}$ and below, the value increased significantly to about $3.0\text{--}5.3 \times 10^{-6} \text{ m}^2 \text{ s}^{-1}$ at $\sigma_\theta = 26.34$. In the region above the target

isopycnal, LDSS estimate an upper limit of $2.4 \times 10^{-6} \text{ W}/\text{kg}$ for the diffusivity in modest agreement with the microstructure values. Below the target isopycnal, LDSS estimate the diffusivity to be in the range of $0.7\text{--}2.1 \times 10^{-6} \text{ W}/\text{kg}$. This result is less than that estimated from the microstructure but within the error bars of our measurements. Using a 3-D model in this more complex region near the bottom boundary layer instead of the 1-D analysis that was done with the dye might have made the comparison better.

4.4. Experiment 2

[38] The comparison between dye and microstructure in this experiment is poor because of difficulties with the dye experiment analysis in separating the dye signal from the background fluorescence. To compound this, problems with EPSONDE (a flooded pressure case) gave a large gap in this data set. Nevertheless, approximately 400 microstructure profiles yielded an estimate of diffusivity. The bottom left inset of Figure 8 shows the microstructure survey centered on DOY 250.1 with a gap followed by the survey centered on DOY 255.0 after the final dye survey. There is an apparent change in the stratification centered at the location of the target surface, with the stratification weaker near the end of the experiment. This experiment had the lowest buoyancy frequency of the four experiments ($N = 6.2$), at a mean depth of 30.5 m, because it was carried out shortly after the passage of Hurricane Edouard. It yielded the largest value of diffusivity ($0.57\text{--}1.47 \times 10^{-5} \text{ m}^2 \text{ s}^{-1}$) that our group measured during the CMO experiment. This is lower than but consistent with the upper limit of $3 \times 10^{-5} \text{ m}^2 \text{ s}^{-1}$ estimated from the dye. Although this is the largest diffusivity measured in CMO, it is no larger than typical oceanic pycnocline values. There is some depth dependence, with K_T becoming smaller as the density increases.

5. Combined Results for All Four Experiments

[39] Because of the ease of measuring velocity microstructure, the eddy diffusivity K_ρ , (equation (2)) is commonly used to express vertical diffusivity. Nevertheless, this requires knowledge of the mixing efficiency, Γ , or more precisely, the flux Richardson number, R_f . In this experiment we measure both the temperature and velocity microstructure and prefer to use the two estimates of vertical diffusivity from equations (1) and (2) to estimate R_f . Rather than using the whole set of microstructure data from the experiment, we use here only the data from the comparison of dye and microstructure. We believe that we have shown that for the most part, the results from these measurements give consistent estimates of mixing from two different techniques. Figure 12 shows values of R_f plotted against the buoyancy frequency, N . In this and in Figures 13, 14, and 15, symbols identify the four experiments: Experiment 2 (circles), Experiment 3 (squares), Experiment 4 (triangles), and Experiment 5 (diamonds). Solid symbols of each shape denote the result at the target density. Open symbols indicate density levels in the region within two segments above and below the target density. The error bars are the bootstrap estimates of the 95% confidence intervals [*Efron and Gong*, 1983]. Little dependence on N is suggested.

1996: Experiment 2

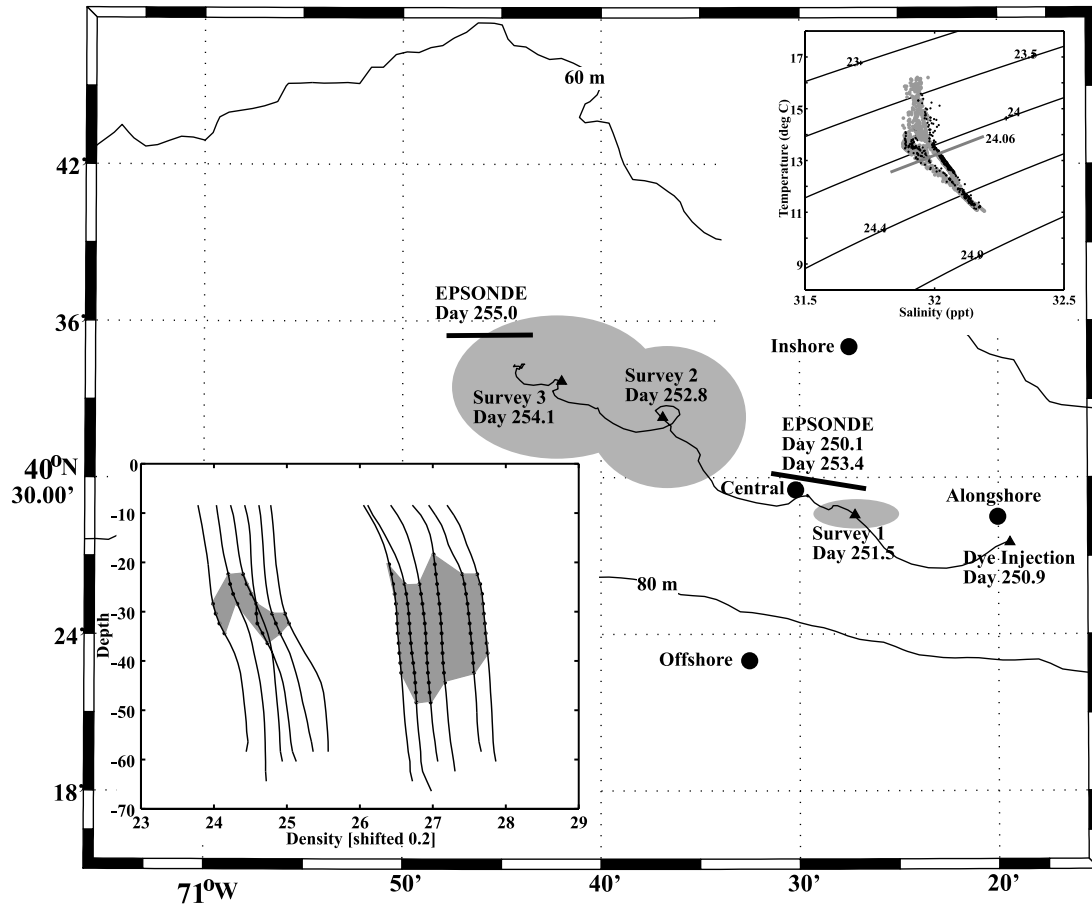


Figure 8. Location of events for CMO Experiment 2 (1996: dye release 1, Rhodamine). This study included the dye injection and three surveys (triangles). Three sets of microstructure data were collected along two lines. The solid line indicates the path of the center of the tracer patch projected between the surveys using hourly ADCP velocities. This line extends beyond survey 3 to the time of the last EPSONDE survey. Shaded ellipses indicate the 4σ extent of the tracer patch in the zonal and meridional directions [Sundermeyer and Ledwell, 2001]. Successive average density profiles are shown for the EPSONDE stations obtained for the microstructure survey in the inset at bottom left. The shaded area represents the range of σ_θ from 23.97 to 24.15 kg/m^3 centered on the target isopycnal at 24.06 kg/m^3 . The blank section in the center is a region in which there were instrument problems. A composite TS plot is shown in the inset at top right. Shaded dots are from EPSONDE, and black dots from the CTD profiles taken at the beginning or end or each EPSONDE line. At the depth of the dye injection at $\sigma_\theta = 24.06$ a difference in TS structure is evident between the start and the end of the experiment.

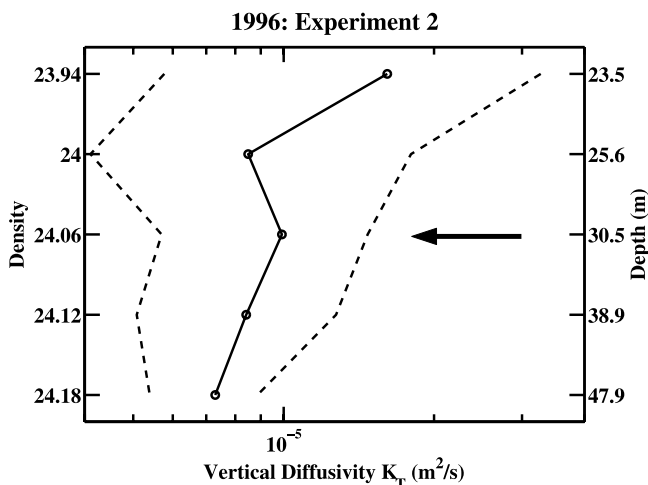


Figure 9. A vertical profile of the vertical diffusivity K_T is shown near the density of the target isopycnal for Experiment 2 (in this case at $\sigma_\theta = 24.06$ near 30 m deep). The labeling and format is the same as for Experiment 4, Figure 5. The vertical mixing rate estimated by the dye is $<3 \times 10^{-5} \text{ m}^2/\text{s}$ as indicated by the arrow.

There are two high values from Experiment 5, which may be related to sampling problems near the strong interleaving interface at the bottom. Ignoring these two points, the mean value $R_f = 0.16 \pm 0.03$. This range is indicated by the two horizontal lines on the figure.

[40] The gradient Richardson number, R_i , and the vertical diffusivity for momentum, K_m , were calculated (equation (4)) by using the velocities measured from the shipboard ADCP in conjunction with the density information from the EPSONDE microstructure profiler. Details of the calculation are given in section 2.4. The calculation of R_i by merging data from two instruments may lead to errors because it is

difficult to match the data in space and time. Each ADCP velocity profile is derived using a vertical bin size of 2 m and time averaging of 3 min. With a ship speed of typically 1 m/s, this represents a horizontal average of order 180 m in the 2-m depth interval. Because we profiled from the stern of the ship with EPSONDE (falling at 0.8 m/s), the microstructure measurement of the dye was typically 50 to 100 m astern of the ship. For this reason, the choice was made to match the ADCP profile closest in time to the EPSONDE profile. Repeating the calculation using the ADCP profile 3 min earlier did not significantly change the estimation of K_m . In the calculation of velocity, the ADCP operation manual (RDI) outlines the weight function for each depth cell. This results in a correlation between adjacent cells of about 15%. Using adjacent cells in the calculation, one might expect an underestimate of the shear. In our calculations, we used the cell above and the cell below the current cell to estimate the shear to reduce this problem at the expense of a coarser resolution in the shear. Using a scale such as the Osmidov scale ($L_{\text{Osmid}} = \sqrt{\varepsilon/N^3}$) to determine the vertical averaging length was not an option since this scale is much smaller than 1 m in most cases in this experiment. The estimates of R_i and K_m for the whole dye experiment were calculated by estimating a value for N^2 , ε , and shear for each station, then, by averaging these station estimates, to obtain a value for the experiment. This estimate captures the shears at inertial and tidal frequencies that probably dominate turbulent production. This allowed us to examine various relationships between mixing parameters and other large-scale parameters. A comparison of R_f versus R_i (Figure 13) suggests little dependence. As in the previous figure, the 95% confidence intervals are shown.

[41] Figure 14 shows that as N increases the ratio K_m/K_T increases also. The same trend is seen in the relationship between K_m/K_T and R_i in Figure 15. Assuming that $K_T = K_\rho$ and examining equations (2) and (4) leads to the equation $K_m/K_T = R_i/R_f$. The data are consistent with the solid line

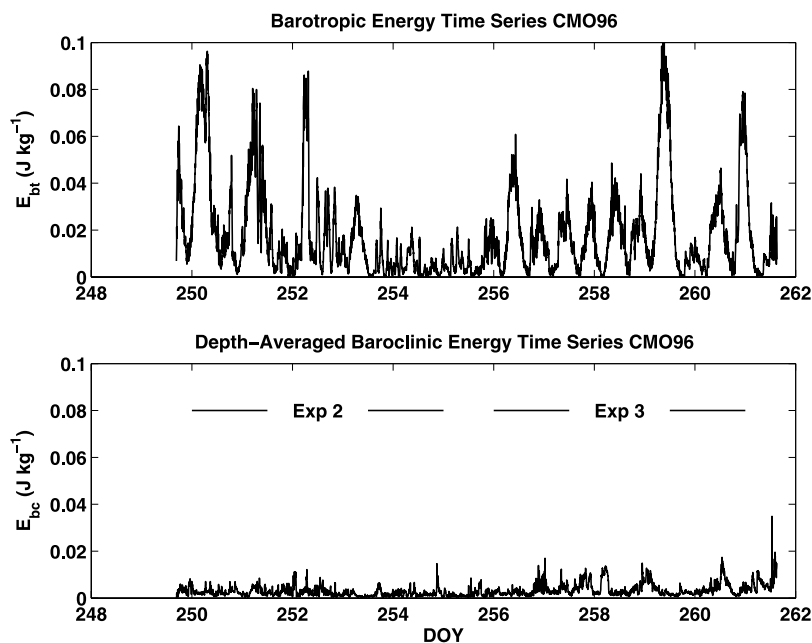


Figure 10. Time series of (top) barotropic and (bottom) depth-averaged baroclinic energy time series derived from shipboard ADCP measurements during September 1996.

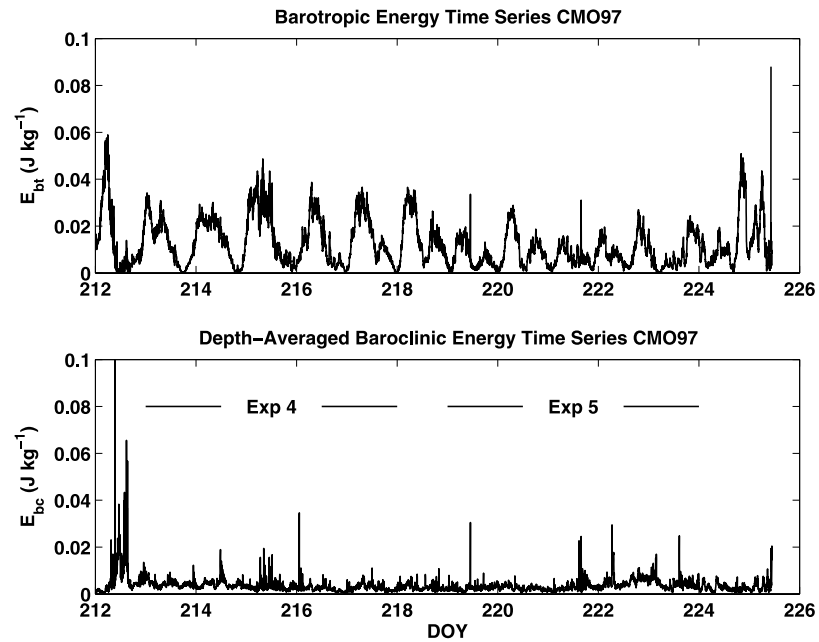


Figure 11. Time series of (top) barotropic and (bottom) depth-averaged baroclinic energy time series derived from shipboard ADCP measurements during August 1997. Curiously, the largest current shown is at the end of the record just before recovery, but since it is well after the dye and microstructure comparison, it has not been investigated.

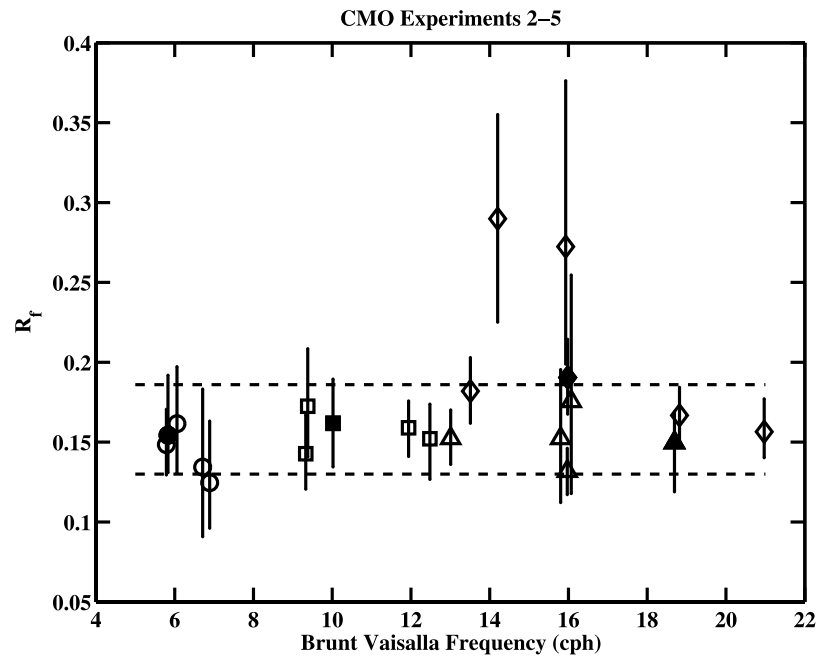


Figure 12. Flux Richardson number is plotted against the Brunt Vaisalla frequency. There are two high values from Experiment 5, but otherwise, there is little dependence seen. Symbols identify the four experiments: Experiment 2, circles; Experiment 3, squares; Experiment 4, triangles; Experiment 5, diamonds. Solid symbols of each shape denote the result at the target density. The horizontal lines at 0.13 and 0.19 represent the 95% confidence intervals (excluding the two extremely anomalous large values).

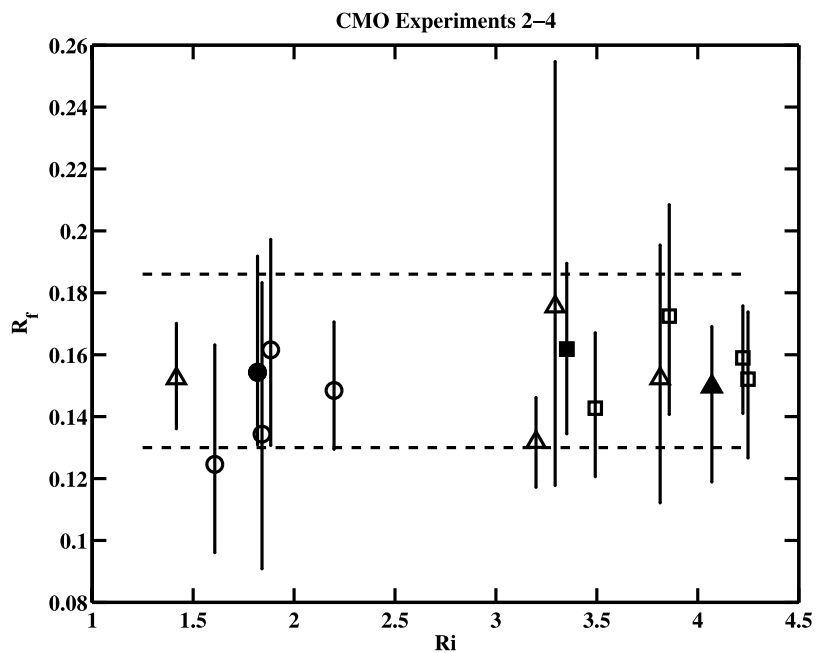


Figure 13. Flux Richardson number is plotted against the gradient Richardson number. Horizontal lines at 0.13 and 0.19 (representing the 95% confidence intervals) suggest little dependence on R_i . Symbols identify the three experiments: Experiment 2, circles; Experiment 3, squares; Experiment 4, triangles. Solid symbols of each shape denote the result at the target density.

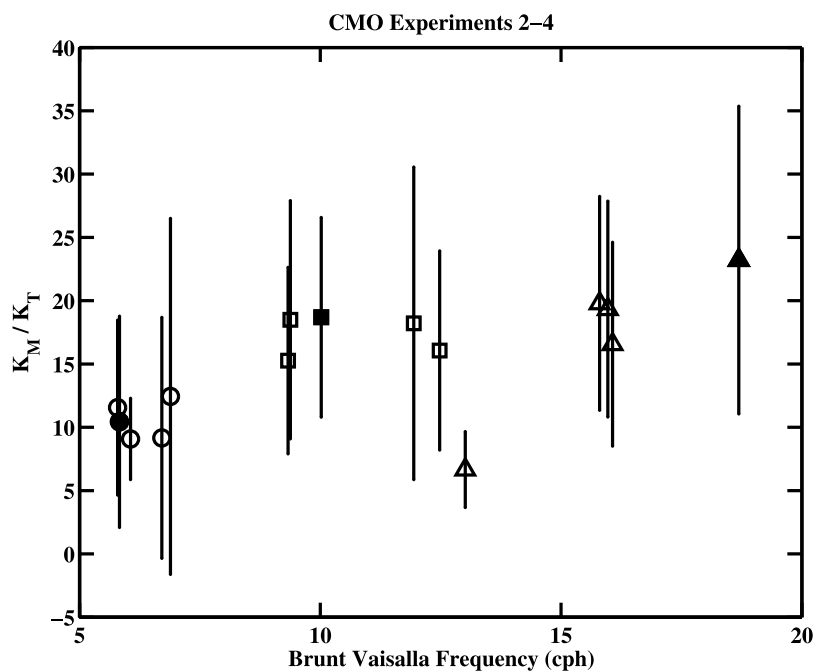


Figure 14. Ratio of vertical diffusivity of momentum and heat is plotted versus the buoyancy frequency. Symbols identify the three experiments: Experiment 2, circles; Experiment 3, squares; Experiment 4, triangles. Solid symbols of each shape denote the result at the target density.

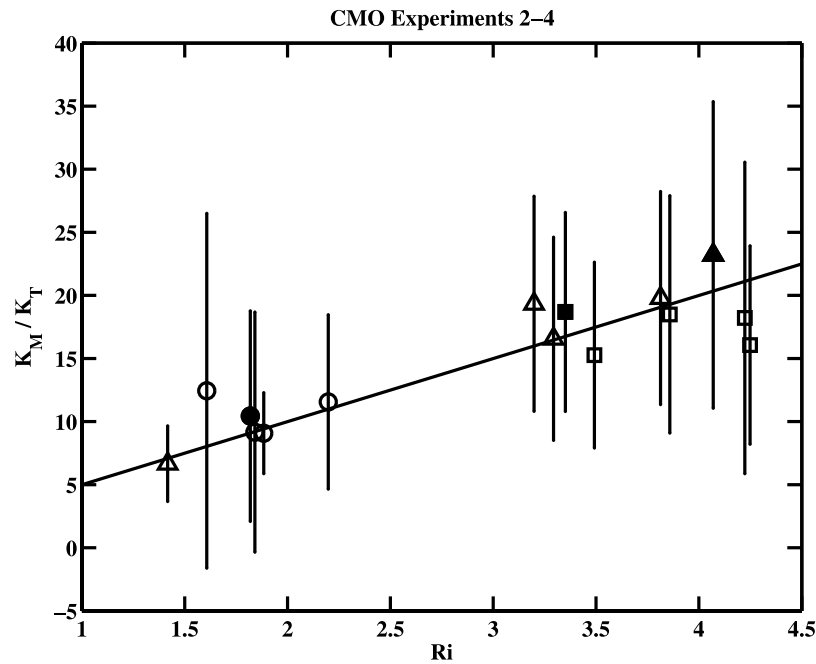


Figure 15. Ratio of vertical diffusivity of momentum and heat is plotted versus the gradient Richardson number. Symbols identify the three experiments: Experiment 2, circles; Experiment 3, squares; Experiment 4, triangles. Solid symbols of each shape denote the result at the target density. The solid line represents the ratio $R_i/R_{f,crit} \approx 5R_i$, where $R_{f,crit}$ is approximately 0.2.

that is plotted for $R_f = 0.2$, often considered a limit for R_f . This is consistent with the observation (Figure 13) that the flux Richardson number that represents the portion of the turbulent energy appearing as a buoyancy flux is largely independent of the gradient Richardson number.

[42] An examination of the summary Table 3 reinforces the result that for almost all of the four experiments, mixing rates were small. Indeed, for Experiments 3 to 5, the Cox number was only about 5. Expressed another way, K_T is only about 5 times the molecular diffusivity of heat. Even in Experiment 2, the Cox number was still only about 20. This resulted in extremely low resultant turbulent heat fluxes of the order a few W/m^2 . The buoyancy modified Reynolds number, $\varepsilon/\nu N^2$ [Dillon and Caldwell, 1980], suggests that when this estimator of turbulent intensity is >200 , turbulence is isotropic. One sees from Table 3 that for

Experiment 2, $\varepsilon/\nu N^2$ is about 52, while for the other three experiments, it is about 11 or 12. Thus one might expect that the simple equations used here to estimate K_T and K_ρ may indeed be incorrect. Yamazaki and Osborn [1990] suggest that the dissipation estimate is comparable to the isotropic estimate for $\varepsilon/\nu N^2 > 20$, but as the value decreases, the error increases, with an underestimate limited to less than 35%. Thus we expect that the estimates of K_T and K_ρ may be underestimated in all but Experiment 2.

6. Conclusions

[43] In this paper, we have presented the results of microstructure measurements of vertical mixing done in conjunction with dye dispersion. Mixing rates from both techniques usually agreed to within the error bars of the

Table 3. Summary of Microstructure Measurements for Experiments 2 to 5^a

| | Unit | Experiment 2 | Experiment 3 | Experiment 4 | Experiment 5 |
|-----------------------|--------------|-----------------------|-----------------------|-----------------------|-----------------------|
| σ_θ range | Kg/m^3 | 23.97–24.15 | 24.15–24.45 | 24.30–24.90 | 25.99–26.29 |
| Depth range | meters | 25.6–38.9 | 42.8–47.4 | 15.9–19.6 | 62.2–64.8 |
| Buoyancy frequency | cph | 6.2 | 10.4 | 16.9 | 16.1 |
| T_z | $^\circ C/m$ | 0.053 | 0.150 | 0.365 | –0.290 |
| ρz | Kg/m^4 | –0.0143 | –0.0398 | –0.1008 | –0.093 |
| K_T | m^2/s | 8.94×10^{-6} | 2.06×10^{-6} | 1.89×10^{-6} | 2.41×10^{-6} |
| K_ρ | m^2/s | 1.34×10^{-5} | 2.94×10^{-6} | 3.09×10^{-6} | 3.09×10^{-6} |
| R_f | | 0.143 | 0.155 | 0.153 | 0.180 |
| Cox number | | 21.3 | 4.89 | 4.43 | 5.27 |
| $\varepsilon/\nu N^2$ | | 51.9 | 11.3 | 11.9 | 11.9 |
| Q_{Heat} | W/m^2 | –2.90 | –1.25 | –2.94 | 3.52 |
| L_{Osmid} | m | 0.348 | 0.134 | 0.110 | 0.119 |
| R_i | | 1.88 | 3.73 | 3.52 | N/A |
| K_m | m^2/s | 1.02×10^{-4} | 3.48×10^{-5} | 3.60×10^{-5} | N/A |

^aThe values quoted are averaged over the region surrounding the target density surface of the dye measurements. N/A means not available.

measurements. Perhaps the most striking thing about these measurements was that mixing was very weak, generally with vertical diffusivities in the range of 10^{-5} to 10^{-6} m^2/s , similar to deep ocean values. This result is in good agreement with *MacKinnon and Gregg* [2003b], who estimated the range of mid-column diffusivity in August 1996 to be $5\text{--}20 \times 10^{-6}$ $\text{m}^2 \text{s}^{-1}$. We have extended the scalar mixing measurements to include the velocity measurements from a shipboard ADCP to calculate the eddy viscosity, K_m , and compared the ratio K_m/K_T to the buoyancy frequency and to the gradient Richardson number. We find a convincing relationship between K_m/K_T and R_i consistent with $K_m/K_T \approx 5 R_i$. Values of $R_f = 0.16 \pm 0.03$ for the flux Richardson numbers are found. These are consistent but slightly lower than those previously found by *Oakey* [1982]. R_f was found to show little dependence on either buoyancy frequency or gradient Richardson number.

[44] **Acknowledgments.** We would like to thank the captain and crew of the RV *Oceanus* for tirelessly helping us in obtaining data with the EPSONDE profiler and for their hospitality during two field programs. We would also like to thank the staff who deployed and recorded the data: Russ Burgett, Dan Clark, Sharon Gillam-Locke, Liam Petrie, Bob Ryan, and Dave Walsh. We would like to thank Harvey Seim and Tim Duda for sharing data with us on the field programs and in particular Jim Ledwell, who coordinated the field programs as Chief Scientist. The program was supported by the Canadian Department of Fisheries and Oceans and by ONR grant N00014-95-1-1030.

References

- Davis, R. E. (1994), Diapycnal mixing in the ocean: The Osborn-Cox Model, *J. Phys. Oceanogr.*, *24*, 2560–2576.
- Davis, R. E. (1996), Sampling turbulent dissipation, *J. Phys. Oceanogr.*, *26*, 341–358.
- Dickey, T. D., and A. J. Williams III (2001), Interdisciplinary ocean process studies on the New England shelf, *J. Geophys. Res.*, *106*(C5), 9427–9434.
- Dillon, T. M., and D. R. Caldwell (1980), The Batchelor spectrum and dissipation in the upper ocean, *J. Geophys. Res.*, *85*, 1910–1916.
- Duda, T. F., and C. R. Rehman (2002), Systematic microstructure variability in double-diffusively stable coastal waters of nonuniform density gradient, *J. Geophys. Res.*, *107*(C10), 3144, doi:10.1029/2001JC000844.
- Efron, B., and G. Gong (1983), A leisurely look at the bootstrap, the jackknife and cross-validation, *Am. Stat.*, *37*, 36–48.
- Gregg, M. C. (1987), Diapycnal mixing in the thermocline: A review, *J. Geophys. Res.*, *92*, 5249–5286.
- Houghton, R. W., and C. Ho (2001), Diapycnal flow through the Georges Bank tidal front: A dye tracer study, *Geophys. Res. Lett.*, *28*, 33–36.
- Ivey, G. N., and J. Imberger (1991), On the nature of turbulence in a stratified fluid: I, The energetics of mixing, *J. Phys. Oceanogr.*, *21*, 650–658.
- Ledwell, J. R., A. J. Watson, and C. S. Law (1998), Mixing of a tracer in the pycnocline, *J. Geophys. Res.*, *103*, 21,499–21,529.
- Ledwell, J. R., T. F. Duda, M. A. Sundermeyer, and H. E. Seim (2004), Mixing in a coastal environment: I. A view from dye dispersion, *J. Geophys. Res.*, C10013, doi:10.1029/2003JC002194.
- Lentz, S., K. Shearman, S. Anderson, A. Plueddemann, and J. Edson (2003), Evolution of stratification over the New England shelf during the Coastal Mixing and Optics study, August 1996 to June 1997, *J. Geophys. Res.*, *108*(C1), 3008, doi:10.1029/2001JC001121.
- MacKinnon, J. A., and M. C. Gregg (2003a), Shear and baroclinic energy flux on the New England shelf, *J. Phys. Oceanogr.*, *33*, 1462–1475.
- MacKinnon, J. A., and M. C. Gregg (2003b), Mixing on the late-summer New England shelf—Solibores, shear and stratification, *J. Phys. Oceanogr.*, *33*, 1476–1492.
- Oakey, N. S. (1982), Determination of the rate of dissipation of turbulent energy from simultaneous temperature and velocity shear microstructure measurements, *J. Phys. Oceanogr.*, *12*, 256–271.
- Oakey, N. S. (1985), Statistics of mixing parameters in the upper ocean during JASIN phase 2, *J. Phys. Oceanogr.*, *12*, 1662–1675.
- Oakey, N. S. (1988), EPSONDE: An instrument to measure turbulence in the deep ocean, *IEEE J. Oceanic Eng.*, *13*, 124–128.
- Osborn, T. R. (1980), Estimates of the local rate of vertical diffusion from dissipation measurements, *J. Phys. Oceanogr.*, *10*, 83–89.
- Osborn, T. R., and C. S. Cox (1972), Oceanic fine structure, *Geophys. Fluid Dyn.*, *3*, 321–345.
- Osborn, T. R., and W. R. Crawford (1980), Turbulent velocity measurements with an airfoil probe, in *Instruments and Methods of Air-Sea Interaction*, edited by L. Hasse, F. Dobson, and R. Davis, Plenum, New York.
- Rehman, C. R., and T. F. Duda (2000), Diapycnal diffusivity inferred from scalar microstructure measurements near the New England shelf/slope front, *J. Phys. Oceanogr.*, *30*, 1354–1371.
- Ruddick, B. R., D. Walsh, and N. Oakey (1997), Variations in apparent mixing efficiency in the North Atlantic central water, *J. Phys. Oceanogr.*, *27*, 2589–2605.
- Sherman, J. T., and R. E. Davis (1995), Observations of temperature microstructure in NATRE, *J. Phys. Oceanogr.*, *25*, 1913–1929.
- Sundermeyer, M. A., and J. R. Ledwell (2001), Lateral dispersion over the continental shelf: Analysis of dye release experiments, *J. Geophys. Res.*, *106*, 9603–9621.
- Yamazaki, H., and T. Osborn (1990), Dissipation estimates for stratified turbulence, *J. Geophys. Res.*, *95*, 9739–9744.

B. J. W. Greenan and N. S. Oakey, Department of Fisheries and Oceans (Canada), Bedford Institute of Oceanography, Dartmouth, Nova Scotia, Canada B2Y 4A2. (greenanb@mar.dfo-mpo.gc.ca)